Tutorial for UVCS CME Observations

This file gives a brief overview of the UVCS instrument and the diagnostics available for CMEs. More details about the instrument are available in Kohl et al. (1997, Sol. Phys. 175, 613) and Gardner et al. (in *The Radiometric Calibration of SOHO*, A. Pauluhn, M.C.E. Huber and R. von Steiger, eds. (ISSI: Bern), p.161)

An overview of UVCS CME observations is included in the review of UV observations of the corona by Kohl et al. (2006, A&A Rev., 13, 31)

CONTENTS

1. UltraViolet Coronagraph Spectrometer 3

2. Observing CMEs with UVCS 4

3. UV Spectra of CMEs 5

4. Examples of CME Spectra 6

5. Making CME Images using UVCS Spectra 7

6. Comparing WL and UV Images 8

7. Diagnostics

I. Doppler Shift 9

II. Line Width 11

III. Doppler Dimming (outflow speed) 12

IV. Density 13

V. Temperature 14

8. Caveats

I. Saturation 15

II. Grating Ghosts 16

III. Grating Scatter

IV. Wires 17

V. Wavelength Scale

VI. Radiometric calibration in second order

VII. Low sensitivity regions on the detectors 18

9. Interpretation 19

1. UltraViolet Coronagraph Spectrometer

The **UVCS** was designed for spectroscopic diagnostics of temperatures, densities, and flow velocities in the extended solar.

The instrument images the corona through an entrance slit 42' long and up to 84" wide, which can be pointed at any polar angle and heliocentric distance from 1.5 to 10 $R_\odot$

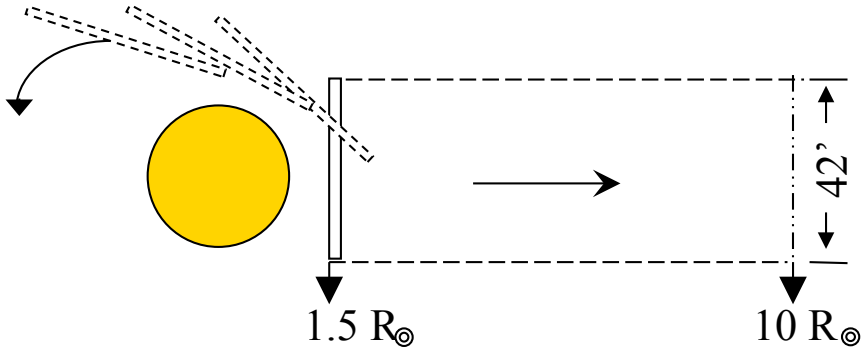

It contains two UV spectrometers (LYA and OVI channels) detecting emission lines in the 950–1350 Å wavelength range. The Table below gives an overview of the UVCS characteristics, for more details see Kohl et al. 1995 and Kohl et al 2006.

Spatial : pixel size 7" (~ 0.01 $R_\odot$)

Spectral	**LYA**	**OVI**	**OVI Redundant**
1° order	1150 – 1350Å	940 – 1120 Å	1160 - 1270
2° order		470 – 560 Å	580 - 635
pixel	0.14 Å	0.1 Å	0.09 Å

2. Observing CMEs with UVCS

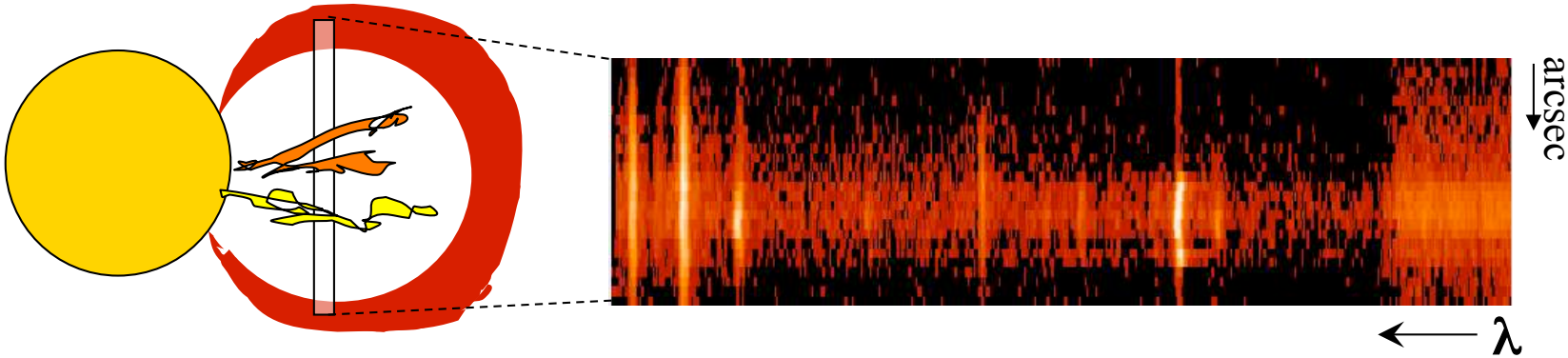

Observation of a CME requires placing the entrance slit at the right time and location in the corona to get spectra of the event as it crosses the FOV of the slit. The spectra are two-dimensional images where the vertical axis is the coordinate along the entrance slit (arcsec or PA) and the horizontal axis is the wavelength dispersion direction.

Spectral resolution ranges from 0.18 to 0.6 Å. The highest resolution is used in the CME watch observations, while the lowest are often obtained during synoptic scans.

A CME can, in principle, be detected at more the one heliocentric distance.

A summary of the characteristics of most CME observations is:

Exp. Time:	CME watch 100 – 200 sec; Synoptic 100 – 600 sec
Heights :	1.5 up to 6 $R_\odot$
Spatial Binning :	21” up to 70” (full detector)
Spectral Lines :	H I Lyman lines (Lyα, Lyβ, Lyδ, Lyγ), C III 977
	N III, O V, OVI(1032,1037), Si XII, Fe XVIII

3. UV Spectra of CMEs

As a CME enters the slit, line intensity changes are detected in the spatial and spectral directions.
In general, the spectra emitted by different parts of the CME are different.
In the context of a three part CME with a front, a void and a bright cavity,
UVCS more often observes the core material and void than the front.

- The core (see **Fig 1**) is highly structured material in terms of knots/threads and Doppler shifts, and it is typically seen in cold lines such as C III 977Å, Si III 1206 Å, Lyman lines etc. However the are a few events in which the core material has been detected in hotter lines.

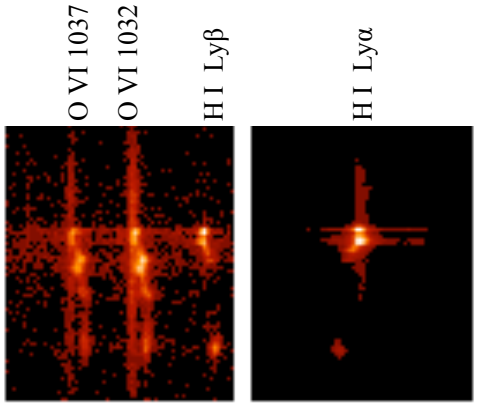

Fig. 1 – The CME core material

- The void is a dimming in the pre-CME coronal emission.

- The front (see **Fig. 2**) is detected as faint and broad emission often in O VI and Si XII lines.

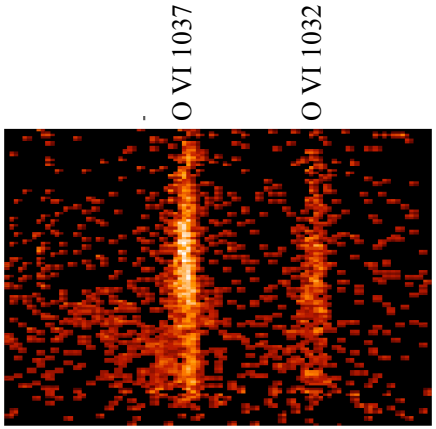

Fig. 2 – The CME front.
(Ciaravella et al 2005,ApJ,621)

4. Examples of CME Spectra

As with white light images, CME spectra can look very different one from another dependingon the morphological and physical characteristics of the CME.

Thus fast, halo CMEs have different spectra from slow ones. Here a streamer blowout spectral sequence is shown on the left and a movie of a halo CME on the right.

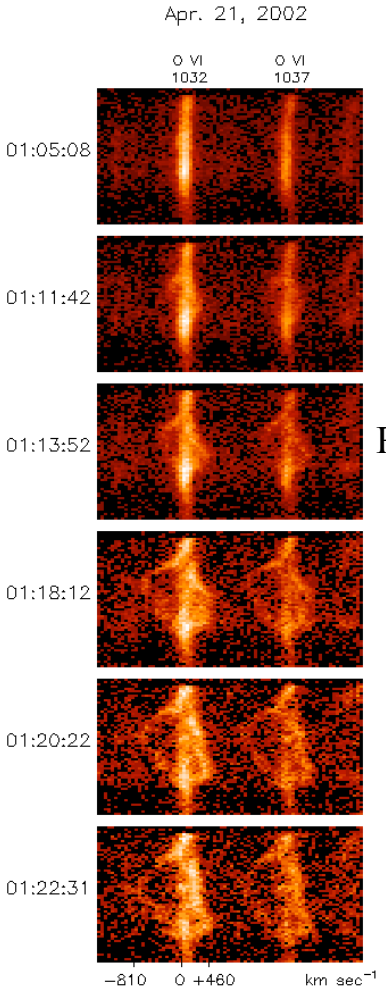

Pre-CME corona

Initial streamer blowout

Red & Blue Doppler shift

(Raymond et al 2003,ApJ,597)

Click on the image to see the evolution of the O VI lines as a CME goes through the UVCS slit

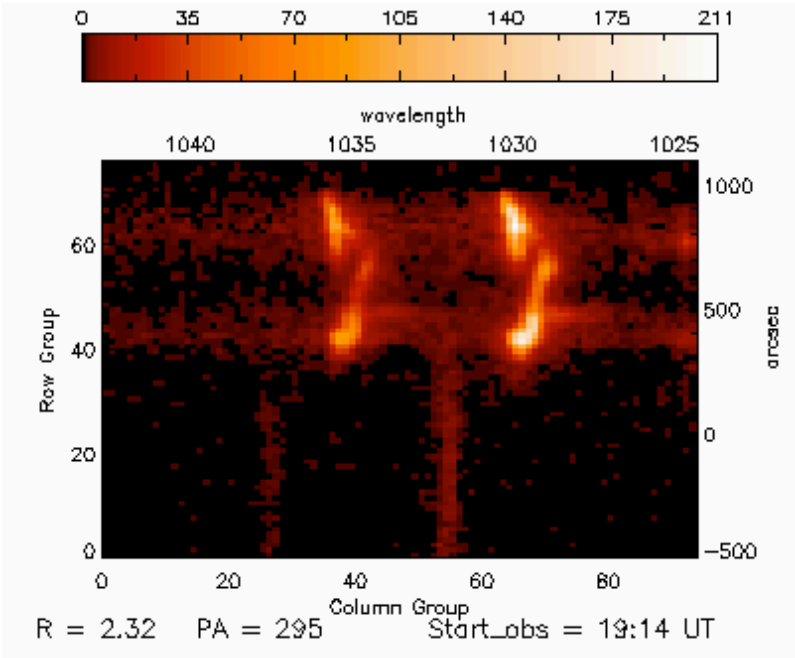

(Ciaravella et al 2005,ApJ,621)

5. Making CME Images using UVCS Spectra

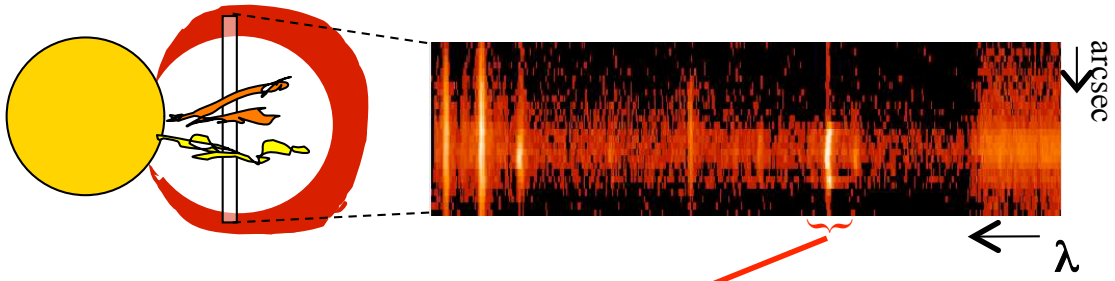

1) As the CME passes though the slit, UVCS collects spectra with a selected spectral range and exposure time

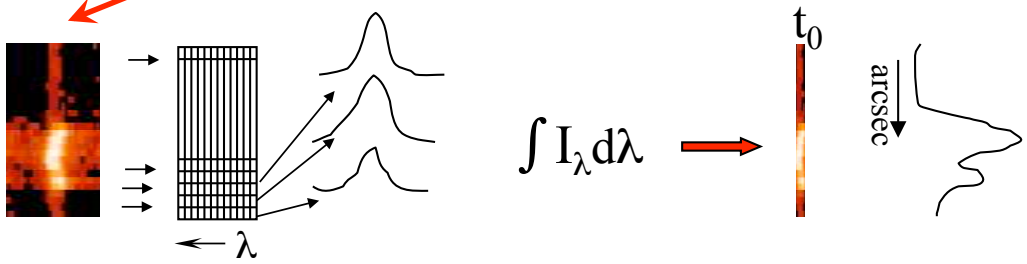

2) Select the spectral line in which CME material is detected and integrate the line profile for each exposure and for each spatial bin to obtain one dimensional images giving the spatial distribution of the line intensity along the entrance slit

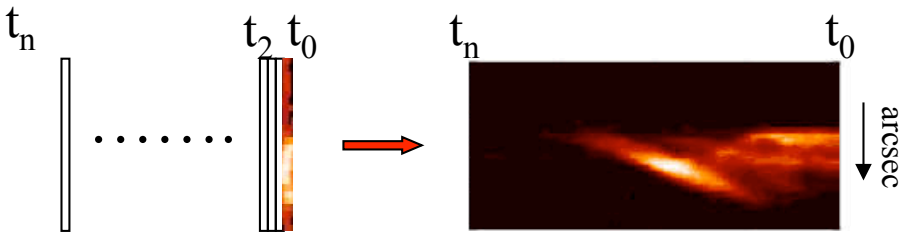

3) By placing the one-dimensional images from consecutive exposures along a time-reversed axis, we obtain an image. The image is then a temporal scan of the event at a fixed position

6. Comparing WL and UV Images

Images of the CME in different spectral lines show that morphology depends on the physical characteristics of the ejecta.

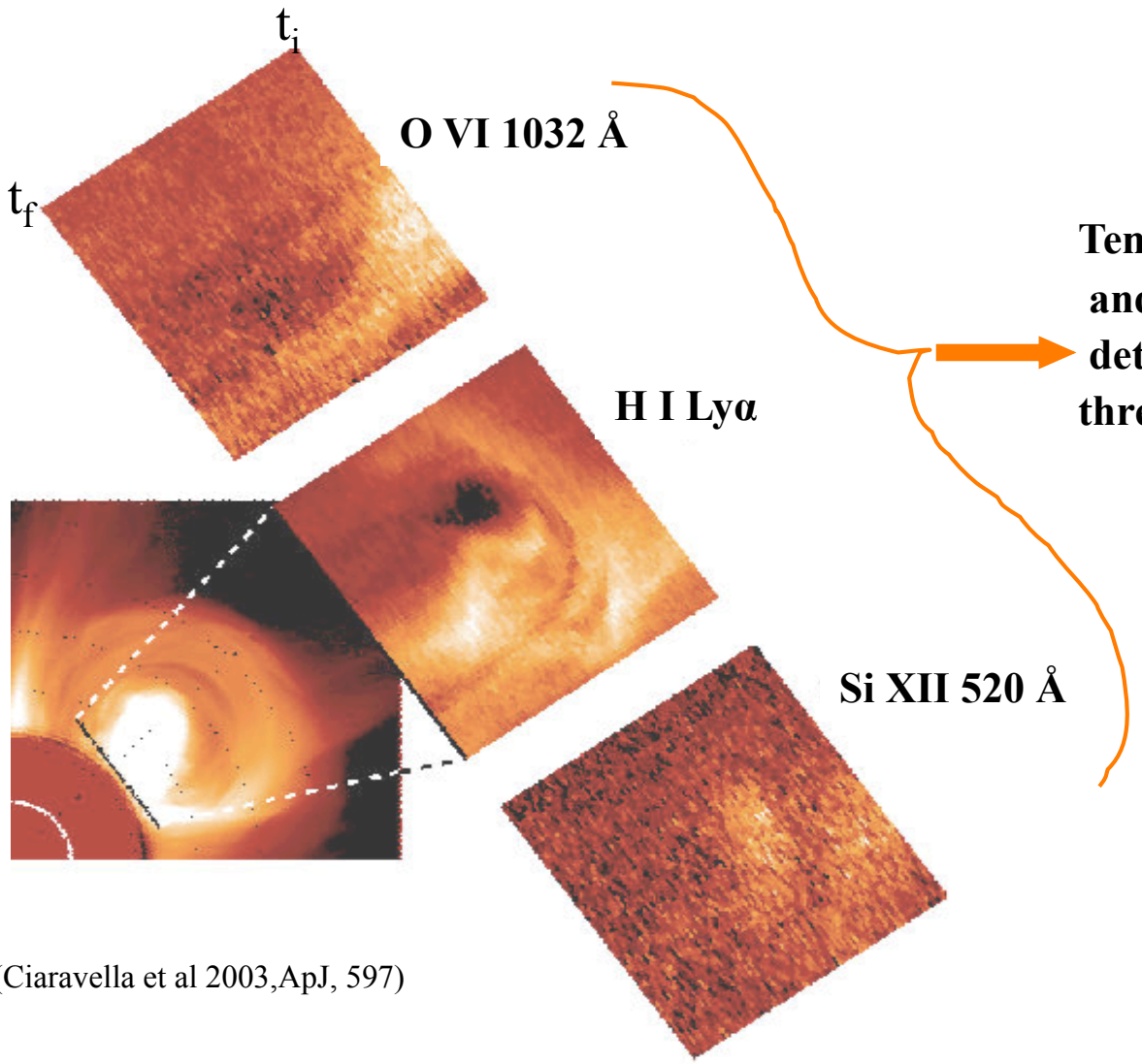

Temperature, density, outflow speed and abundances of the ejected plasma determine the morphology in the three selected spectral lines.

t_i = beginning of the observation
t_f = end of the observation

(Ciaravella et al 2003,ApJ, 597)

Diagnostics: I. Doppler Shift

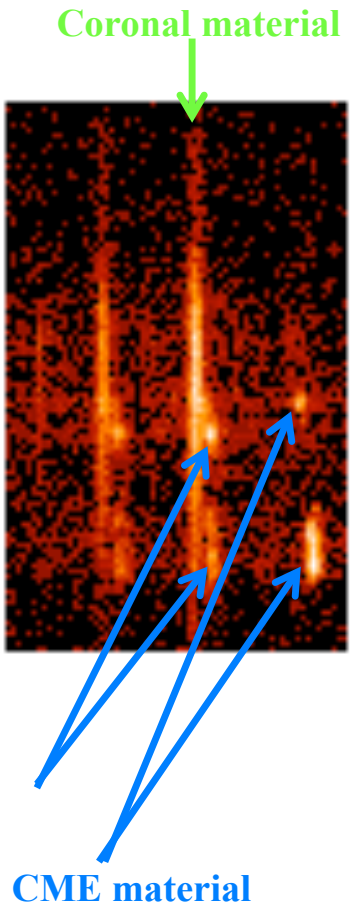

Doppler shift of the spectral lines provides the line of sight speed of the emitting material.

In the spectrum on the left the CME material on the right of the background coronal emission is blue shifted.

In particular for :

Collisional lines → $w_{LOS} = \frac{\Delta\lambda}{\lambda} \times c$

Radiatively Excited Lines

(Noci & Maccari, 1999, A&A, 341)

$$v_{LOS} = \frac{(q^2 + \sin^2\phi) w_{LOS} + b\cos\phi}{q^2 + 1}$$

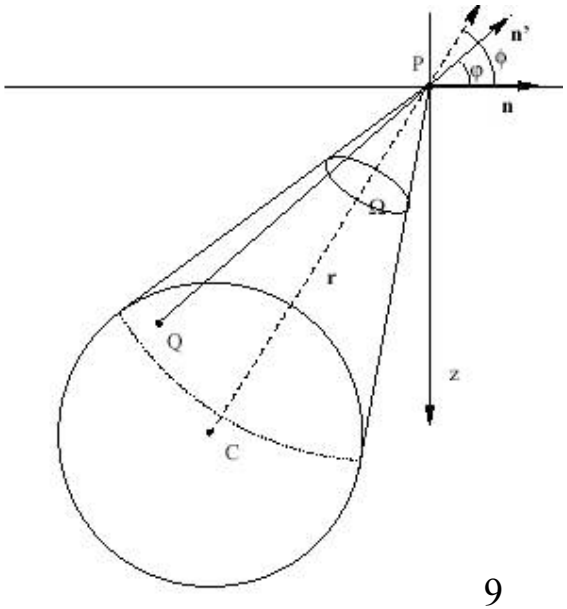

7. **Diagnostics I.** Doppler Shift cont

1997 Dec 11

The Doppler shift evolution suggests a helical motion of the ejecta.

Spatial structure and the LOS velocity evolution were interpreted as a

Left-Handed helix untwisting at $\sim 9 \times 10^{-4}$ rad /sec

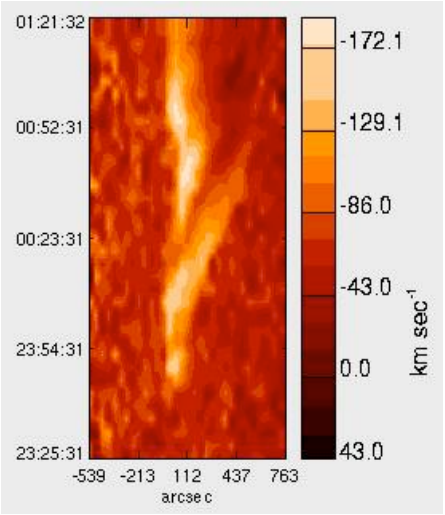

(Ciaravella et al 2000,ApJ,529)

2000 Feb 12

The front was moving toward the Earth at speed varying from 10 km/sec in the southern leg to 60 km/sec in the northern leg.

The core shows along its S shape a smooth change from blue (-30 km /sec) to red shift (+25 km /sec)

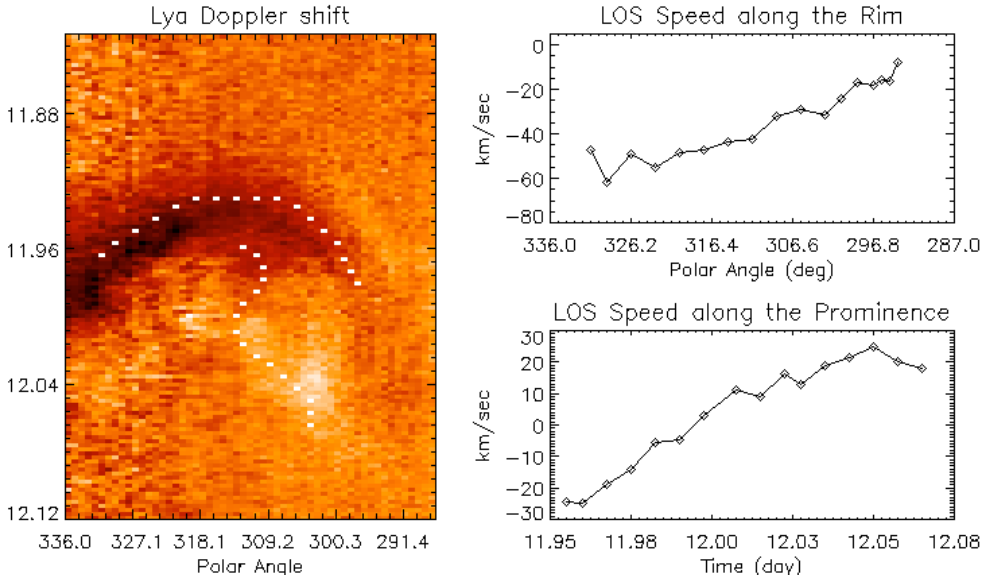

(Ciaravella et al 2003,ApJ, 597)

Diagnostics II. Line Width

The analysis of line profiles provides diagnostics of **ion temperature** (see pag . 13) as well as **bulk speed** of the emitting plasma. Both increasing temperature and expansion of the emitting material contribute to broadening the line profiles. The comparison of different spectral lines and the estimate of the expansion speed are required to disentangle the two effects (Ciaravella et al. 2005, ApJ, 621; Raymond et al. 2000, GeoRL, 27).

The **passage of a shock** heats the emitting material and is detected as broad wings mainly in the non neutral ions. The mechanisms responsible for heating the neutral atoms , such as ionizing collisions with the hot electrons of the plasma or resonant charge transfer with fast shocked protons, require long time scales. Thus, in the UVCS spectra the presence of a shock front is more likely to be detected in the spectral lines of the brightest ions such as the O VI doublet, but broadening of the H I Lyα line, if present, provides a direct diagnostic of the proton temperature behind the shock. Detections of shocks in UV spectra have already been reported for four CMEs (Raymond et al. 2000 ,GeoRL, 27 ; Mancuso et al. 2002, A&A, 383; Raouafi et al. 2004, A&A, 424 ; Ciaravella et al. 2005, ApJ, 621; Mancuso & Avetta 2008, ApJ, 677, 683).

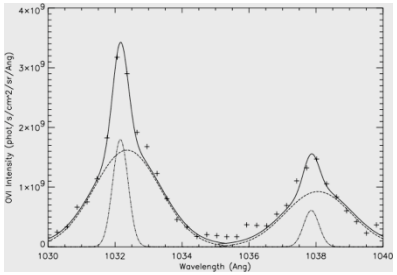

Broad wings in the O VI doublet as results of a shock passage (from Mancuso et al. 2000, A&A).

Diagnostics III. Doppler Dimming (outflow speed)

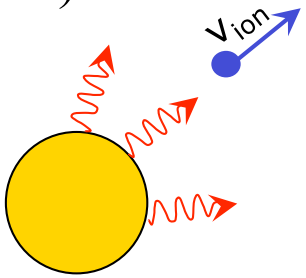

UV spectra provide a method to estimate the outflow speed by using the spectral lines with radiative components, such as the **O VI 1032, 1037 Å** doublet. The collisional components of the O VI lines have an intensity ratio of 0.5, while the ratio of the radiative components is 0.25 for emitting plasma at rest. The radiative component originates from the resonant scattering of the chromospheric line by the O VI ions of the corona. The intensity of the radiative component depends on the speed of the scattering ion .

As the ions move outward in the corona, the radiative component dims because the solar emission and coronal absorption profiles are Doppler shifted apart.

Thus, the line ratio increases and eventually becomes collisional when the outflow speed is such that the absorbing and emitting profiles no longer overlap.

However, at higher speeds the nearby lines of C II 1036.34, 1037.02 Å can pump the radiative component of the 1037 Å line at outflow speeds of 170 and 370 km/sec, respectively.

In very fast CMEs pumping of the 1037 Å line by 1032 Å (v = 1650 km/sec) and the 1032 Å line by Lyβ (v =1810 km/sec) can occur, as for the 2000 June 28 event (Raymond & Ciaravella 2004, ApJ, 606).

Diagnostics IV. Density

Diagnostics of density can be obtained from different spectral lines.

- The **O VI doublet** provides diagnostics of density (Mariska 1977 , Ph. D Thesis; Noci et al. 1987, ApJ , 315; Raymond & Ciaravella 2004, ApJ, 597). Since the illuminating flux from the disk is known, the intensity of the radiative component fixes the number of O VI ions in the corona. The intensity of the collisional component, combined with the O VI column density and excitation rate, determines the electron density. This is most easily applied to pre-CME coronal densities, but it can sometimes be used for CME ejecta.

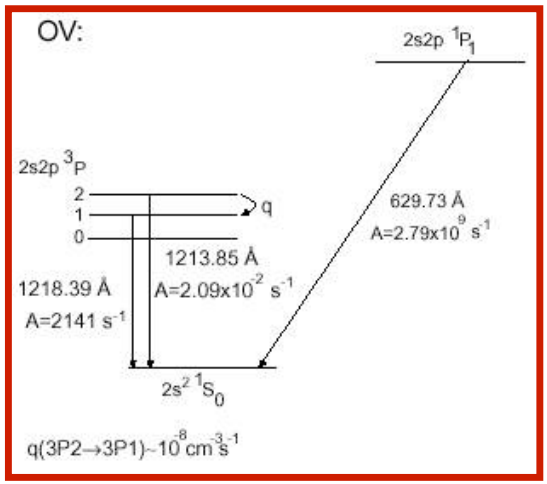

- The ratio of the intensities of the **[O V]** forbidden line at **1213.85 Å** and the **O V]** intercombination line at **1218.39 Å** provides a reliable density diagnostic. The forbidden line is generally difficult to detect in solar spectra, since it occurs within the wing of the bright Lyα line. This ratio has successfully been used to determine the electron density of the 1999 April 23 CME at heliocentric height of 3.5 R (Akmal et al. 2001, ApJ, 553). The density determination is based on transitions between the triplet P excited state and the singlet S ground state. Near the critical density $\boldsymbol{n_c}$ the P_2 state is depopulated via collision in favor of the P_1 state. The critical density is:

$$n_c = \frac{A(^3P_2 \rightarrow {}^1S_0)}{q(^3P_2 \rightarrow {}^3P_1)} \approx 10^6\, cm^{-3}$$

$A =$ radiative decay rate

$q =$ collisional rate coefficient

Diagnostics V. Temperature

The lines in the observed spectra indicate the **ionization stage** and the range of temperatures of the emitting material. The table lists the maximum temperature of formation of the some of the most common lines in UVCS spectra in ionization equilibrium. At the larger heights and in faster CMEs, ionization equilibrium may not hold.

Spectral Lines	$\mathbf{T_{Max}}$
Lyα, Lyβ, Lyδ, Lyγ	1.3×10^4
C III, Si III, N III	$4 - 8 \times 10^4$
S V], N V, O VI	$1.6 - 3 \times 10^5$
[S X], Si XII, [Fe XVIII]	$1.3 - 6.8 \times 10^6$

The **ion temperature** can be obtained from the line width:

$$\frac{\Delta\lambda}{\lambda} = \frac{v}{c} \qquad v = \sqrt{\frac{2KT}{M}}$$

Comparison of observed and predicted line ratios provide diagnostics of the **electron temperature**:

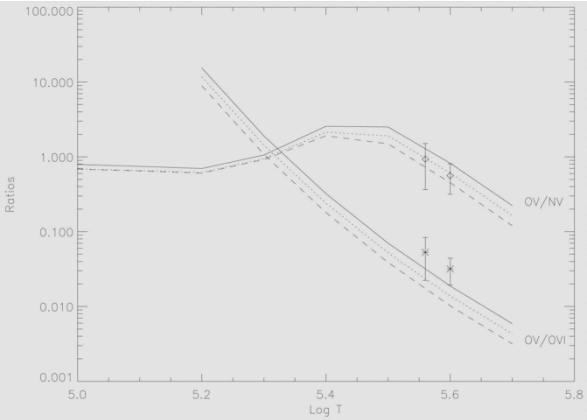

Predicted O V]/O VI and O V]/N V line ratios as a function of the temperature, and density of 10^6 cm^{-3} (solid line),10^7 cm^{-3} (dotted line), and 10^8 cm^{-3} (dashed line). The diamonds and asterisks are the observed values with their error bars . From Ciaravella et al., 1999, ApJ, 510 .

8. Caveats

I. Saturation

CMEs can be far brighter than the quiet corona that UVCS was meant to observe, and the brightest lines can become saturated. The most critical problem generally occurs for HI Lyα and Lyβ, C III 977 Å, and one or two other bright lines. This saturation has not been calibrated for UVCS. To give an idea of the magnitude of the effect, we show the loss of sensitivity as a function of count rate for the nearly identical detectors of SUMER (from the SUMER ssw package *idl/contrib/wilhelm/corr/local_gain_corr.pro*)

Rate	Sensitivity
0.0	1.0
0.1	1.0
0.3	0.99
1.0	0.986
3.0	0.928
10.	0.866
30.	0.765
100.	0.500
300	0.123

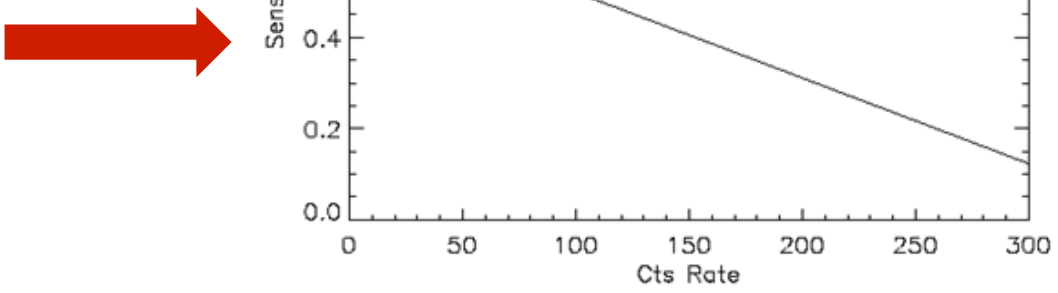

Note that these are counts per pixel per second.

UVCS data are usually binned by 3, 6 or more pixels.

Caveats Cont.

II. Grating Ghosts

Imperfections in the diffraction grating can cause spurious images of a bright line at other wavelengths, particularly in the O VI channel. Pre-flight laboratory measurements showed ghosts at ±28.5Å from a strong line in the LYA channel. The most troublesome ghosts in the OVI channel arise from Lyα even when that line is not on the detector:

λ	$I/I_{Ly\alpha}$
987.85	$1.3x10^{-4}$
1011.08	$1.0x10^{-4}$
1033.03	$1.1x10^{-4}$
1052.96	$8.5x10^{-5}$
1079.35	$4.0x10^{-4}$
1170.00	$\sim 1.0x10^{-3}$
1261.33	$\sim 1.0x10^{-3}$

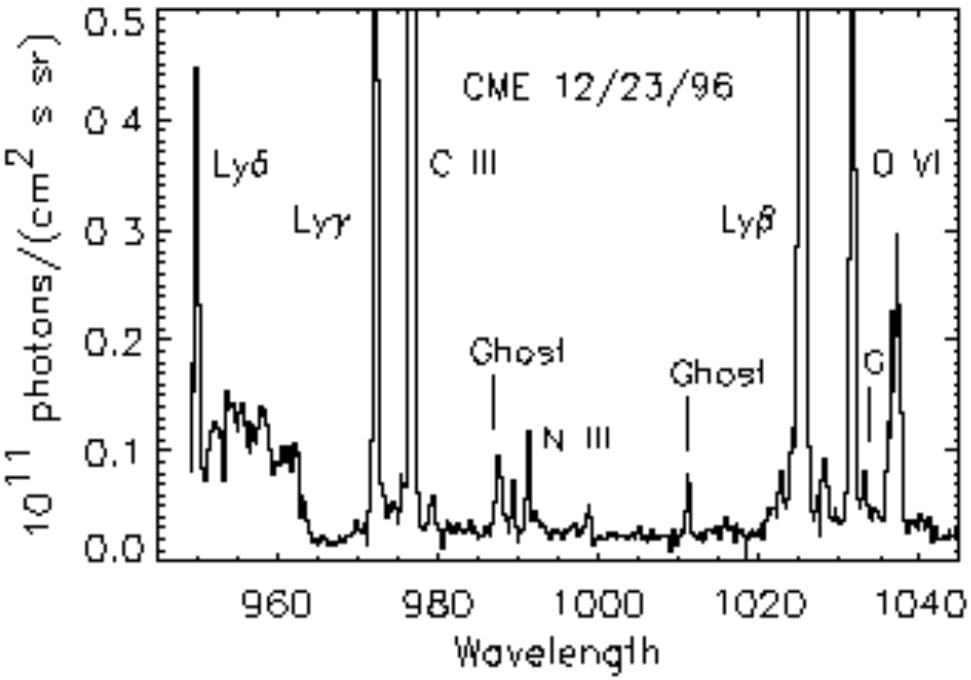

Caveats Cont.

III. **Grating Scatter** (false continuum)

Roughness in the conventionally ruled grating in the OVI channel scatters photons along the dispersion direction. The example shown is from the **1996 Dec 23** CME (Ciaravella et al. 1997, ApJ, 491). Note that the pseudo-continuum is twice as bright at the right hand end, where light from the redundant mirror is added to the direct illumination.

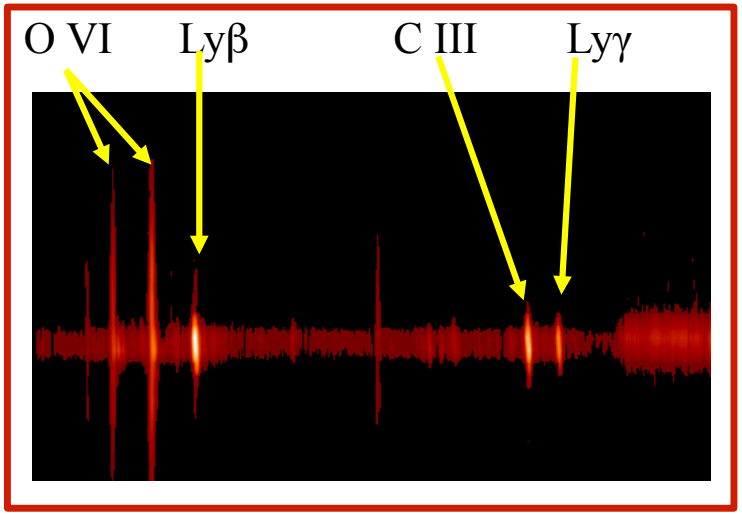

IV. **X-ray artifacts**

……

……

V. **Particles background**

……

……

9. Interpretation

The catalog includes a set of subjective assessments of the likelihood that a given event shows indications of a shock wave, a current sheet, or other interesting phenomenon based on a quick look at the data.

The criteria used are:

- **Front**

The UVCS slit has the position and temporal coverage to catch the CME Front, and some change in the line profile or intensity is seen.

- **Void**

The CME Void generally appears as just a lack of emission, and it is hard to discriminate between emission from the void and emission from the front and back of the bubble. In general, Void is indicated if some change in the ionization state or line profile suggested emission from the interior of the CME.

- **Shock**

A shock is indicated by very broad O VI line profiles when the Leading Edge crosses the slit.

Interpretation Cont.

- **Current Sheet**

Emission in [Fe XVIII] λ974 after the CME onset is taken as an indication of a current sheet, especially if it is seen in a narrow region along the slit and if it lasts for a long time.

- **Prominence**

Bright emission in low stages of ionization such as C III and N III is taken to how ejected prominence material, particularly when these lines occur in small spatial regions.

- **Flare OVI**

O VI emission all along the slit before the CME material arrives at the slit indicates flare O VI photons scattered by O VI ions in the corona.

- **Leg**

Fairly bright emission in low ionization lines (e.g., C III) that lasts for a long time and has little Doppler shift is interpreted as a flux filament connecting the CME back to the Sun.

- **Helix**

A filament or strand that moves along the UVCS slit and also moves in Doppler shift may indicate a helical motion, but detailed models are needed to verify this interpretation.